International Journal of Earth Sciences (2022) 111:1273–1287
https://doi.org/10.1007/s00531-022-02179-0

ORIGINAL PAPER

The detrital zircon record of Variscan to post-Variscan tectonosedimentary and magmatic processes in the Tauern Window (Eastern Alps)

P. Veselá[1] · S. Oriolo[2,3] · M. A. S. Basei[4] · B. Lammerer[1] · S. Siegesmund[3]

Received: 6 September 2021 / Accepted: 24 February 2022 / Published online: 19 March 2022

Abstract
Coupled U–Pb and Lu–Hf LA-ICP-MS detrital and igneous zircon data were obtained from metasedimentary sequences (Kaserer Formation, Schmirntal Quartzite, Seidlwinkel Formation, Bündnerschiefer Basin, Riffler Basin) of the western Tauern Window (Eastern Alps). Results show maximum deposition ages between the Late Permian and the Triassic, indicating protracted sedimentation and magmatism between the Late Paleozoic and the Mesozoic. The Lu–Hf fingerprint shows a change from subchondritic to variable subchondritic to suprachondritic compositions at ca. 290 Ma, possibly documenting the transition from Late Paleozoic Variscan post-collisional processes to intracontinental extension. Lithospheric thinning and magmatic underplating may explain the observed Hf isotopic evolution as the result of mixing of crustal and mantellic sources. From a paleogeographical perspective, results confirm that the Tauern Window was situated between Alpine basement units (South Alpine, Austroalpine and External Massifs) and the Bohemian Massif during the Permian–Triassic.

Keywords Alpine basement · Variscan orogeny · Penninic ocean · Permian–Triassic intracontinental rifting · Lu–Hf isotopes · Pangea break-up

Introduction

After Paleozoic accretionary processes linked to protracted subduction, the basement of the proto-Alps underwent significant deformation and metamorphism during the Variscan Orogeny (e.g., von Raumer et al. 2009, 2013; Siegesmund et al. 2021). Towards the Permian, a transition from Variscan post-collisional processes to continental extension related to Pangea break-up is recorded, giving rise to high-temperature/low-pressure metamorphism coupled with rifting-related magmatism (Marotta and Spalla 2007; Schuster and Stüwe 2008; Quick et al. 2009; Kunz et al. 2018; Manzotti et al. 2018; Yuan et al. 2020). Protracted crustal extension during the Triassic favoured the development of rift basins and associated magmatism (e.g., Doglioni 1987; Satterley 1996; Kurz et al. 1998; Veselá et al. 2008, 2011; Storck et al. 2019; De Min et al. 2020), cultiminating in the final Jurassic opening of the Penninic ocean (Ratschbacher et al. 2004; Gleißner et al. 2021).

The Variscan to post-Variscan tectonic evolution of the proto-Alps is particularly well-recorded in the Tauern Window (Lammerer et al. 2008; Schmid et al. 2013). Devonian to Carboniferous Variscan tectonometamorphic and magmatic processes were succeeded by Permian–Triassic rifting-related basin development and magmatism (Söllner et al. 1991; Eichhorn et al. 1999, 2000; Cesare et al. 2002; Kebede et al. 2005; Veselá and Lammerer 2008; Veselá et al. 2008, 2011; Siegesmund et al. 2021). Rifting ended in the Late Jurassic, with deposition of platform carbonates and the final separation of the European and Adria plates.

✉ S. Oriolo
seba.oriolo@gmail.com; soriolo@gl.fcen.uba.ar

1 Department of Earth and Environmental Sciences, Ludwig-Maximilians-Universität München, Luisenstraße 37, 80333 Munich, Germany

2 Instituto de Geociencias Básicas, Aplicadas y Ambientales de Buenos Aires (IGEBA), CONICET-Universidad de Buenos Aires, Intendente Güiraldes, 2160, C1428EHA Buenos Aires, Argentina

3 Geoscience Centre, Georg-August-Universität Göttingen, Goldschmidtstraße 3, 37077 Göttingen, Germany

4 Centro de Pesquisas Geocronologicas, Instituto de Geociências, Universidade de São Paulo, Rua do Lago 562, São Paulo 05508-080, Brazil

In this contribution, new U–Pb and Lu–Hf detrital zircon data of Permian–Triassic metasedimentary sequences of the Tauern Window are presented. Maximum sedimentation ages and provenance are discussed, providing constraints on Permian–Triassic paleogeography of Alpine basement domains and adjacent crustal blocks. In addition, insights into Variscan to post-Variscan crustal growth and tectonosedimentary evolution of the Tauern Window are evaluated.

Geological setting

The Tauern Window occupies a central position in the orogenic architecture of the Eastern Alps. The lowermost stratigraphic sequences can be found here, including the pre-Alpine European basement and its sedimentary cover, albeit significantly overprinted by metamorphism and deformation (Fig. 1; e.g. Frasl 1958). From a structural perspective, the Tauern Window is formed by a duplex structure in the centre of the Eastern Alps, which underwent up to ca. 35 km of Alpine burial and exhumation caused by N–S crustal shortening and E–W extension during indentation of the Adriatic plate (Selverstone 1985, 1988; Selverstone et al. 1984, 1995; Rosenberg et al. 2007; Ratschbacher et al. 1989; Frisch et al. 2000; Lammerer et al. 2008; Schmid et al. 2013). Basement and cover rocks of European plate provenance (Inner Tauern Window) and oceanic origin (Glockner nappe) are stacked together and subsequently folded (Figs. 2 and 3), favoured by anistropic layering due to granitoid sill and laccolith intrusions (Höck and Miller 1980; Lammerer and Weger 1998).

The post-Variscan intramontane basins were filled with coarse- to fine-grained clastic sediments and acid volcanic rocks (Eichhorn et al. 2000; Veselá et al. 2008, 2011). During the post-rift subsidence, the Late Jurassic Hochstegen limestone covered the entire region (Kiessling 1992). A comparable situation can be found in the northern foothills of the Alps, where it is documented in deep boreholes (Lemcke 1988). In this context, the tectonostratigraphic position of rocks exposed in the hanging wall of the Hochstegen limestone, namely the Kaserer Formation (metaquartzites, metarkoses, schists, breccias and thin metadolomite lenses or layers) and equivalent sequences, is controversial. In short, there are two main proposals:

1. The Kaserer metasedimentary rocks comformably overlie the Hochstegen limestone, implying a sedimentary contact and therefore a Cretaceous age of the former (Frisch 1974; Rockenschaub et al. 2003; Schmid et al. 2013).
2. The Kaserer metasedimentary rocks are overthrust as a nappe system. In this case, rocks may be older, being originally deposited further south but still within the European margin of the Penninic ocean. In this case, the Kaserer Formation would be somehow related to the Permian–Triassic Haselgebirge, Verrucano and Buntsandstein formations and even to the continental to shallow marine Bellerophon and Werfen sequences of the Northern Calcareous Alps and the Southern Alps (Fenti and Friz 1973; Tollmann 1977; Baggio et al. 1982).

Materials and methods

Samples were collected for coupled U–Pb and Lu–Hf LA-ICP-MS zircon analysis, comprising mainly metasedimentary sequences from the basal Glockner Nappe (BSF, FMA, SMQZT, TXQZT, MSTG), the Kaserer Nappe (MSBG, KAS), the Riffler basin (MKG) and one metaigneous rock (TXRH), which marks together with metagabbro lenses the thrust plane of the Glockner Nappe. Sample locations are shown in Fig. 2, whereas sampling site coordinates are detailed in Supplementary Material 1. Approximately 3–5 kg for each sample were crushed and disintegrated using disc mill to obtain a grain fraction between ca. 50–500 µm. The size fraction < 315 µm was processed using the Wilfley table to concentrate the heavy minerals. The heavy fraction of the samples was loaded to sodium polytungstate and subsequently to diiodomethane heavy liquids, followed by removal of the magnetic minerals using the Frantz isodynamic separator. Zircons were arranged in rows, cast into epoxy resin discs having a diameter of 2.54 cm, and polished to reveal grain centres. Prior to analysis, cathodoluminescence and transmitted light images were obtained so that the best sites for analysis could be chosen. Zircon analyses were performed using a Neptune multicollector inductively coupled plasma mass spectrometer (ICP-MS) and an Analyte G2 excimer laser ablation (LA) system at the University of São Paulo (Brazil). Analytical results of U–Pb and Lu–Hf data are presented in Supplementary Materials 2 and 3, respectively, whereas details on analytical procedures are included in Supplementary Material 4.

An overview of the studied samples is presented in Table 1. Sample MKG corresponds to a metaconglomerate to meta-arenite of the Riffler Basin, which is tectonically the lowermost unit. For the metasedimentary Kaserer Formation, sample KAS was collected; it corresponds to a brownish calcareous metaquartzite, intercalated with a graphitic phyllite. MSBG comprises a graphitic micaschist of the Seidlwinkl Formation, collected from the footwall the Glockner Nappe thrust, which is marked by the mylonitic orthogneiss of sample TXRH. Graphitic micaschists (MSTG) and chlorite-muscovite-bearing metaquartzites (TXQTZ) were sampled in the hanging wall of the Glockner Nappe thrust (Fig. 2). Sample SMQZT (Schmirntal Quartzite) comprises a white metaquartzite, whereas FMA

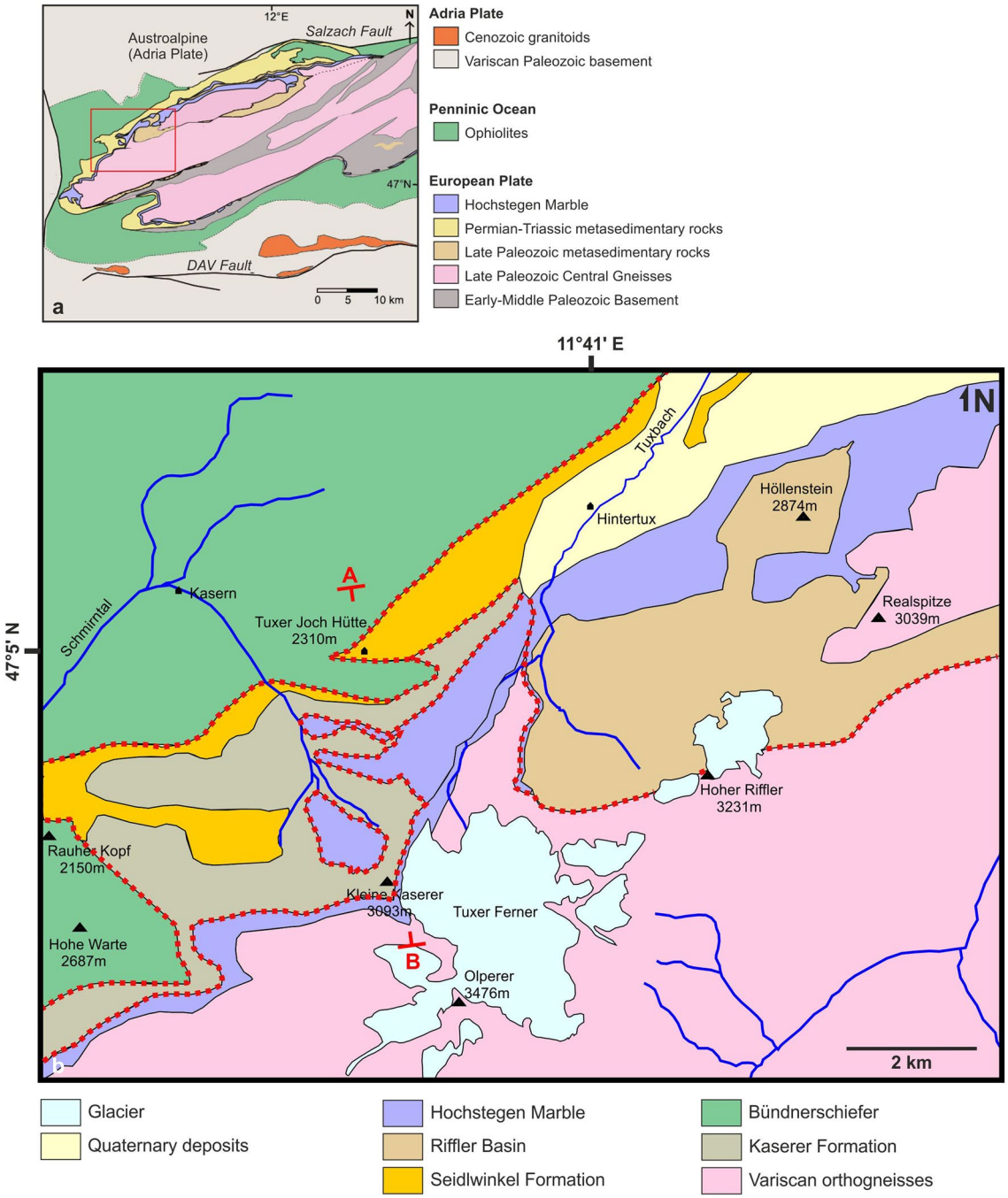

Fig. 1 **a** Regional sketch map of the western Tauern Window. Red area shows location of map of **b**. **b** Detailed geological map of the study area. The A–B profile depicts the geological section of Fig. 2a. Thrusts are indicated with red dotted lines

is a fine-grained phengitic meta-arkose, so far attributed to the Wustkogel Formation (Thiele 1976) but more likely corresponding to the Seidlwinkel Formation (see "Age and provenance"). Finally, a black sandy phyllite with calcareous layers (BSF) was sampled close to the base of the Bündnerschiefer unit of the Glockner Nappe.

Results

U–Pb LA-ICP-MS

Maximum sedimentation ages for metasedimentary rocks were obtained following three approaches, i.e., youngest

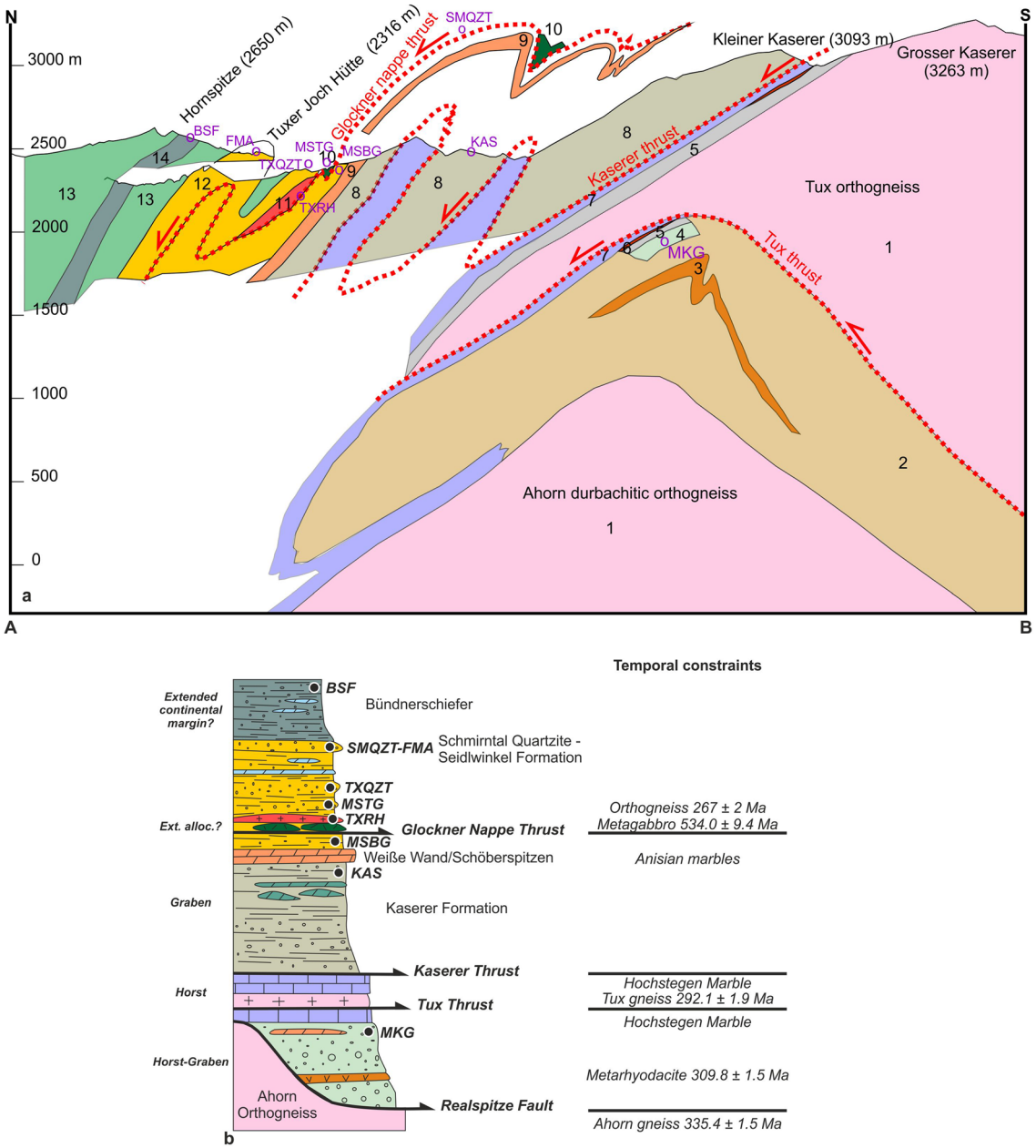

Fig. 2 **a** Regional geological profile showing units and sampling location. For samples collected to the west and east of the profile, their location is schematically depicted above or below the main profile (e.g., samples SMQZT, MKG). 1: Variscan orthogneisses, 2 and 4: Riffler Basin metasedimentary rocks with intercalation of (3) late Carboniferous metarhyodacite, 5: grey metaquartzites and metaconglomerates, 6: brown sandy marbles, 7: Hochstegen Marble, 8: Kaserer Formation, 9: middle Triassic dolomitic and calcareous marbles, 10: metagabbro, 11: metarhyolite, 12: mixed metasiliciclastic-carbonatic sequences (Seidlwinkel Formation), 13: Bündnerschiefer with intercalation of (14) black schist. **b** Schematic stratigraphic section showing samples and age constraints. Geochronological data from this work and Veselá et al. (2008, 2011)

detrital grain (YDG), youngest grain cluster at 1σ (YGC1) and youngest grain cluster at 2σ (YGC2) (Table 1; Dickinson and Gehrels 2009; Coutts et al. 2019). In all cases, calculations were made considering $^{206}Pb/^{238}U$ ages, since the youngest zircons of all samples yield Late Paleozoic to Triassic ages. All calculations of the youngest cluster weighted mean age were based on $n=2$ and $n=3$ for ages overlapping at 1σ and 2σ, respectively. In some samples, scarce zircons yielded anomalously young ages (< 210 Ma) which seem to record Pb loss and are thus not considered for estimation of sedimentation ages

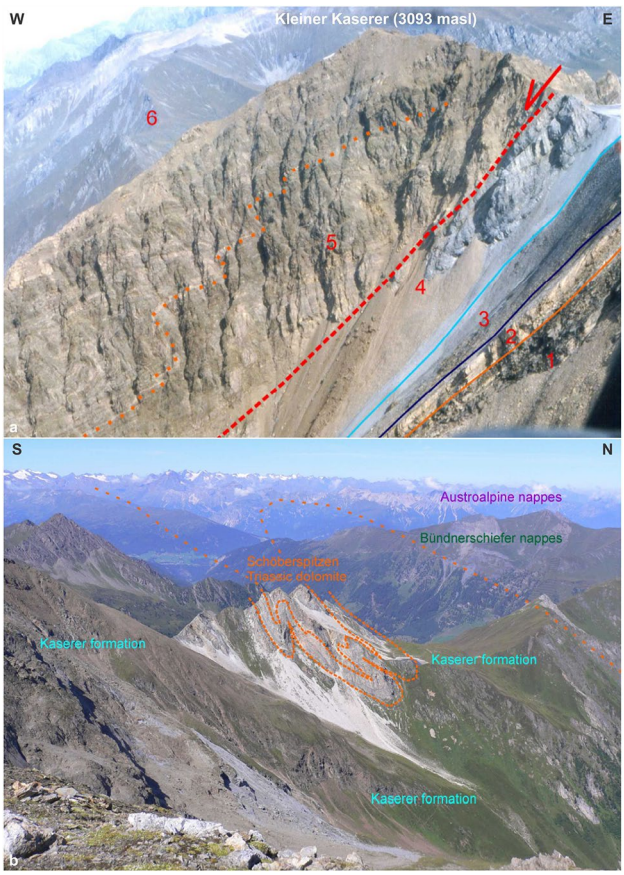

Fig. 3 **a** Type locality of the Kaserer Formation at the Kleiner Kaserer (3093 masl). 1: granitic basement of the Tux gneiss nappe, 2: Middle Triassic (?) dolomitic marbles, 3: Early Jurassic black schists, 4: Hochstegen Marble, 5: folded Kaserer Formation, 6: Bündnerschiefer calc-schists. View from helicopter to the north. **b** Kaserer Formation underlying tightly folded Middle Triassic dolomites of the Schöberspitz. View from the Kleiner Kaserer summit towards the west

(Supplementary Material 2). Results of detrital zircon age spectra are presented in Fig. 4 and Table 1.

Metasedimentary samples commonly show euhedral to subhedral and fragmented zircons, though subordinate subrounded to ovoid crystals are present as well. Internal structures mainly correspond to oscillatory and minor sector zoning, whereas thin homogeneous dark or bright rims are common.

Sample KAS shows a well-defined Guadalupian maximum sedimentation age, based on all parameters (YDG = 267 ± 3 Ma, YGC1 = 268 ± 4 Ma, YGC2 = 269 ± 3 Ma). In terms of provenance, Paleozoic ages are clearly dominant, with main peaks at ca. 480–440 and 320–280 Ma. Scarce Cryogenian and Stenian crystals are also present.

The youngest single grain of sample MSBG yields a late Triassic age of 236 ± 3 Ma and scattered Permian crystals are also present. However, estimations of YGC1 and YGC2 are much older, providing early to middle Devonian ages. The main detrital zircon population corresponds to ages of ca. 455–435 Ma. A minor peak of 580–600 Ma is also recorded, together with subordinate Paleoproterozoic, Stenian and Tonian contributions.

A late Triassic maximum sedimentation age is clear for MSTG, as indicated by the YDG at 207 ± 3 Ma, and slightly older ages of 224 ± 4 and 225 ± 10 Ma of YGC1 and YGC2, respectively. Provenance is dominated by ages of ca. 320–280 Ma and a second peak at ca. 460–440 Ma. A minor group at ca. 560–570 Ma and a few Tonian crystals are present as well.

In the case of sample TXQZTG, a middle to early Triassic age maximum sedimentation age of ca. 250–243 Ma is obtained by all calculations. Two main peaks mainly at ca. 460–430 and 280–260 Ma are observed, though a minor group at ca. 610–580 Ma and three Neoarchean-Paleoproterozoic grains are also recorded.

For sample SMQZT, all parameters point to a comparable late Triassic maximum sedimentation age of ca.

Table 1 Maximum sedimentation and metamorphism ages

Sample	Lithology	Unit	YDG	YGC1	YGC2
KAS	Metaquartzite	Kaserer Formation	267 ± 3	268 ± 4	269 ± 3
MSBG	Micaschist	Seidlwinkel Formation	236 ± 3	392 ± 47	395 ± 17
MSTG	Micaschist	Glockner Nappe metasedimentary rocks	207 ± 3	224 ± 4	225 ± 10
TXQZTG	Metaquartzite	Glockner Nappe metasedimentary rocks	243 ± 5	248 ± 39	250 ± 3
SMQZT	Metaquartzite	Schmirntal Quartzite	232 ± 2	233 ± 3	235 ± 12
FMA	Meta-arkose	Seidlwinkel Formation (Pfiffkar Formation?)	233 ± 3	234 ± 37	240 ± 14
BSF	Phyllite	Bündnerschiefer Basin	266 ± 3	266 ± 5	268 ± 5
MKG	Meta-arenite	Riffler Basin	213 ± 2	241 ± 3	256 ± 9

Ages in Ma, all errors at ± 1σ

YDG youngest detrital grain, *YGC1* youngest grain cluster at 1σ (n = 2), *YGC2* youngest grain cluster at 2σ (n = 3)

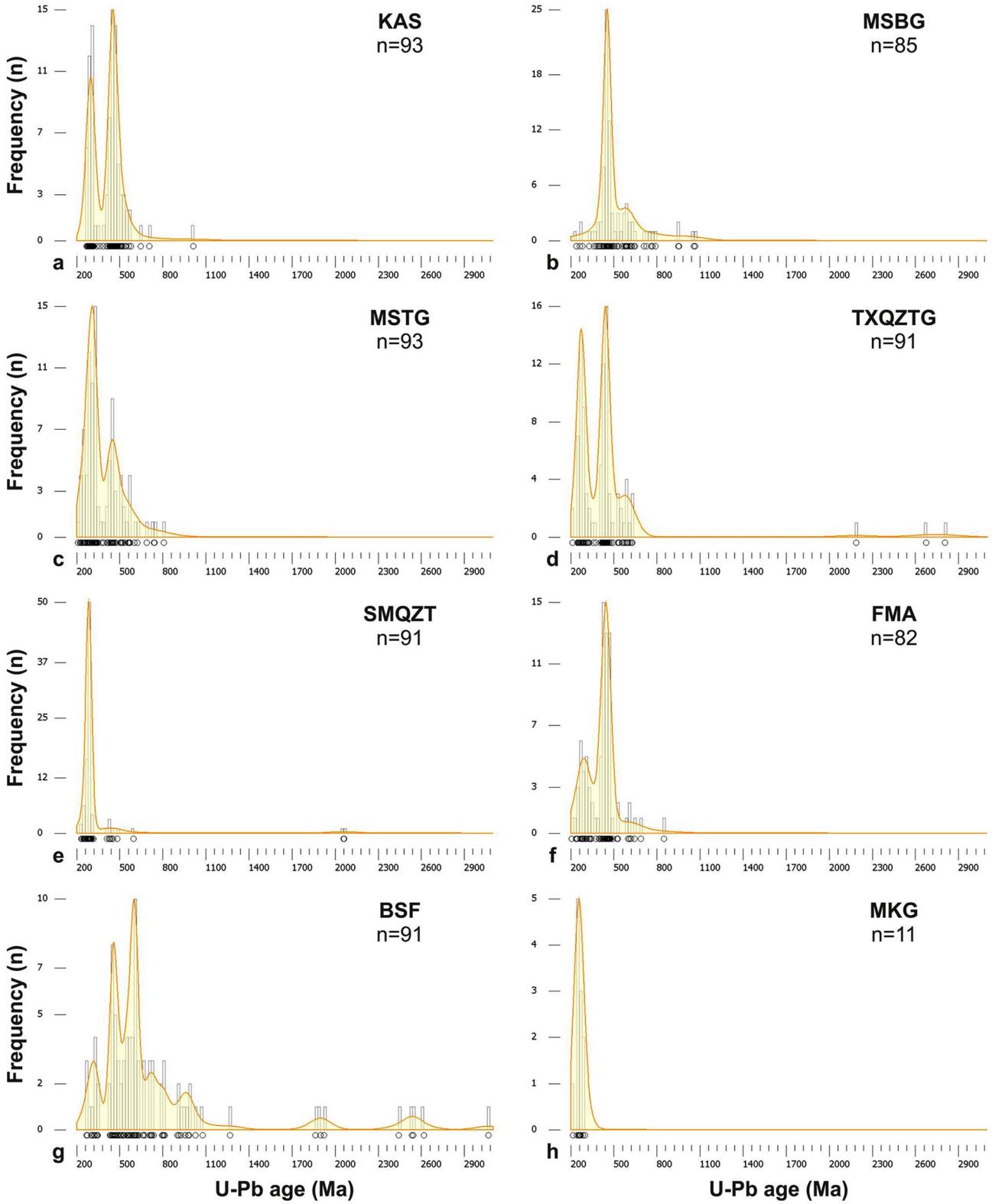

Fig. 4 Kernel density estimate curves and histograms plotted using DensityPlotter (Vermeesch 2012) for U–Pb detrital zircon data results. Plots only include data with ± 10% discordance. Bin and band width = 20 myr

235–232 Ma. Provenance is clearly dominated by early Permian ages, mainly of ca. 290–280 Ma, though a minor contribution of Silurian ages between ca. 440 and 420 Ma is present as well. A Paleoproterozoic and an Ediacaran crystal are also recorded.

Middle to late Triassic maximum sedimentation ages, mainly at ca. 240–233 Ma, are also documented by all three calculations for sample FMA, which is dominated by euhedral to subhedral zircons with oscillatory zoning and dark rims. The main peak corresponds to Ordovician to early Siluarian ages of ca. 480–420 Ma, followed by Late Carboniferous-Permian crystals of ca. 320–260 Ma. A minor contribution of Neoproterozoic zircons is also observed.

Sample BSF yields a very robust middle Permian maximum sedimentation age of ca. 268–266 Ma, indicated by comparable YDG, YGC1 and YGC2 values. Provenance is dominated by an Ediacaran peak at ca. 610–580 Ma, followed by a second Ordovician to early Silurian group at ca. 470–435 Ma. In addition, subordinate contributions of ages of ca. 330–310 and 720–700 Ma, together with scattered Archean to Tonian crystals, are documented as well.

Though only scarce zircons were obtained from sample MKG, they provide a late Permian (YGC2) to middle-late Triassic (YGC1 and YDG) maximum sedimentation age. In a similar way, provenance is restricted to Permian–Triassic crystals, mainly yielding ages of ca. 260–240 Ma.

Finally, euhedral to subhedral zircons of sample TXRH, characterized by oscillatory zoning, yield a concordia age of 267 ± 2 Ma for the timing of crystallization of the felsic orthogneiss protolith (Fig. 5). In addition, the sample shows significant inheritance of xenocrysts, mainly of ca. 325–270 Ma, 460–420 and 620–580 Ma, with further scattered grains yielding Paleoproterozoic, Tonian, Cryogenian and Paleozoic ages (Supplementary Material 2).

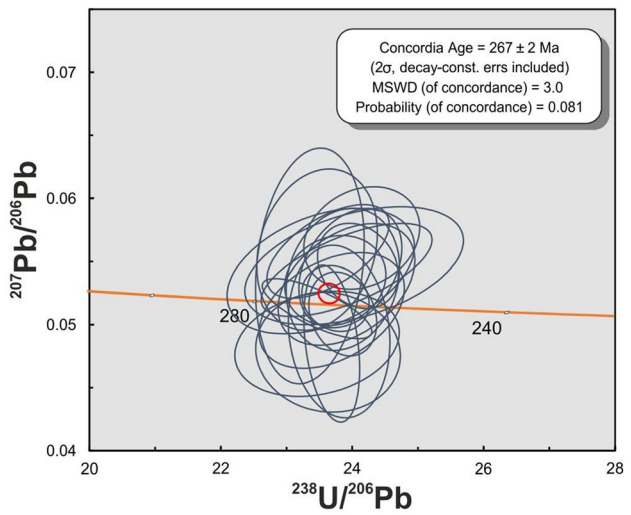

Fig. 5 U–Pb concordia age for the orthogneiss of sample TXRH

Lu–Hf isotopes

Coeval detrital zircons of different stratigraphic units and samples show similar Lu–Hf signature, indicating that no major differences are recorded among them. Such similarities are also observed for xenocrysts of the orthogneiss sample TXRH (Fig. 6). Paleoproterozoic and Stenian-early Tonian zircons yield dominantly subchondritic compositions, with ε_{Hf} below ca. − 4. Though scarce, scattered values between ca. + 6 and − 27 are recorded by late Tonian to Cryogenian crystals. Ediacaran to early Cambrian zircons yield variable compositions between ca. + 7 and − 27 as well. In contrast, the composition of Ordovician to Silurian crystals is almost restricted to subchondritic values between ca. − 4 and − 28.

Carboniferous to very early Permian zircons are dominated by subchondritic compositions, mainly between − 3 and − 11. In contrast, zircons with crystallization ages between the middle Cisuralian (ca. 290 Ma) and the Middle Triassic show a broad compositional spectrum, with ε_{Hf} between + 4 and − 24. They define an apparent bimodal distribution, with a first group dominated by subchondritic values below ca. − 9 and a second cluster with slightly subchondritic to suprachondritic values between ca. + 4 and − 5. The latter group is mainly recorded by zircons of sample TXQZTG and magmatic crystals of sample TXRH.

Discussion

Age and provenance

Despite minor differences, all studied metasedimentary rocks yielded similar results, with maximum sedimentation ages between the late Permian and the Triassic (Table 1). The Guadalupian maximum sedimentation age of sample KAS is in line with correlations of the Kaserer Formation upper section with Anisian rocks of the Wolfendorn area (Frisch 1975; Veselá et al. 2008). Consequently, a late Permian to early Triassic deposition age is inferred. Even though a Cretaceous age for the Kaserer Formation cannot be completely ruled out, there is no evidence for the suspected Cretaceous age. In contrast to previous proposals (e.g., Frisch 1975; Thiele 1976; Rockenschaub et al. 2003; Schmid et al. 2013), a tectonic contact between the top of the Upper Jurassic Hochstegen Marble and the Kaserer Formation is assumed (Fig. 3), further supported by field evidence, such as different folding styles and local sheared gypsum lenses at the contact (e.g., Steinernes Lamm crest), and a conformal contact with the Middle Triassic carbonates at the Schöberspitz and other locations. In addition, the Late Triassic maximum deposition age for the overlying MSBG sample (Fig. 2) reinforces this interpretation.

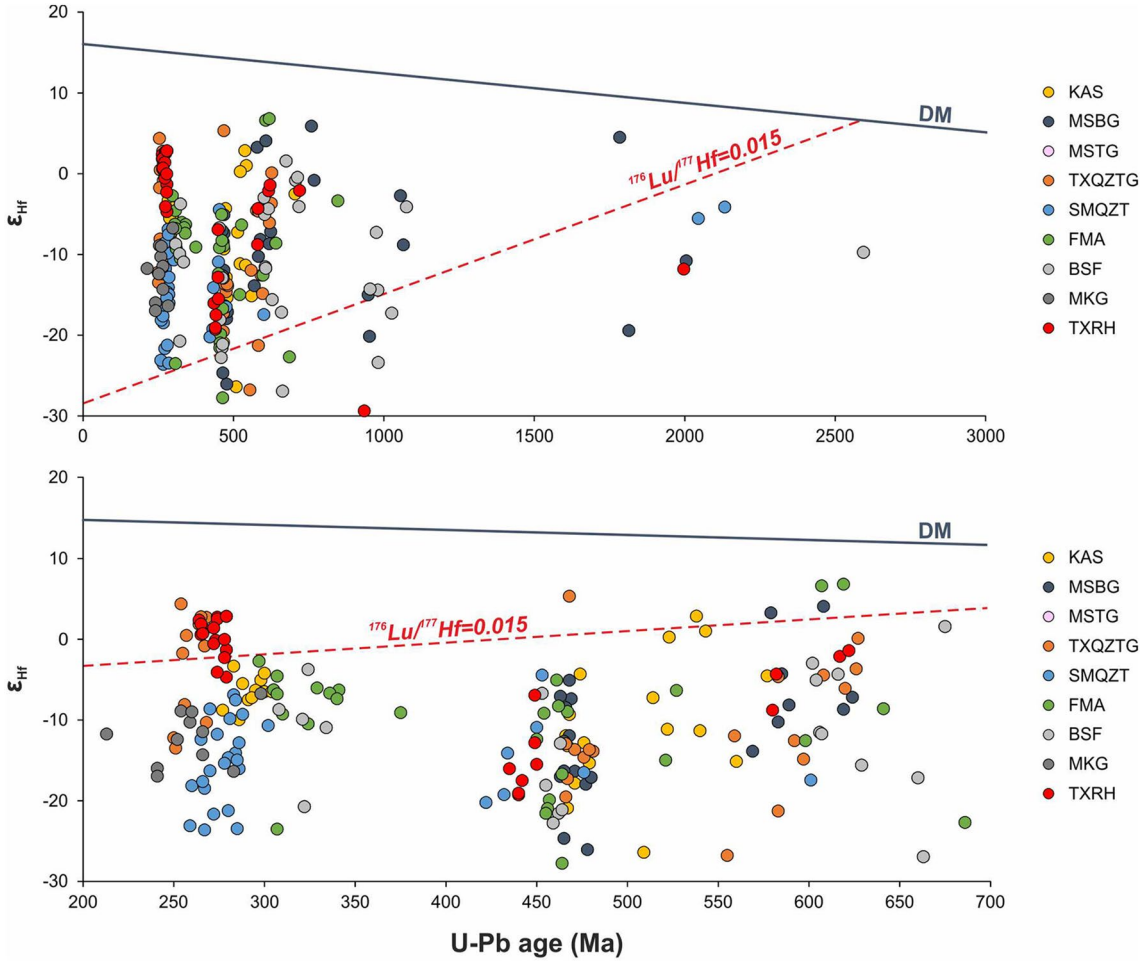

Fig. 6 U–Pb vs. ε_{Hf} data of studied units. The lower diagram shows a detail of age distribution for zircons < 700 Ma. Data were recalculated considering a constant decay λ $^{176}Lu = 1.867 \times 10^{-11}$ year^{-1} (Söderlund et al. 2004) and CHUR values of $^{176}Hf/^{177}Hf = 0.282785$ and $^{176}Lu/^{177}Hf = 0.0336$ (Bouvier et al. 2008). The red line indicates a crustal array with $^{176}Lu/^{177}Hf = 0.015$, typical for a crustal reservoir (e.g., Vervoort and Blichert-Toft 1999)

On the other hand, metasedimentary rocks of the Glockner Nappe, which are spatially associated with tectonic slices of Cambrian metagabbros and Permian orthogneisses at the base (Fig. 2b, Veselá et al. 2008), yielded middle to late Triassic maximum sedimentation ages (samples MSTG, TXQZT, SMQZT, FMA). This may indicate that, though these rocks may be part of the Triassic clastic sedimentary sequences of the area, they may represent slightly younger deposits than those of the Kaserer Formation sensu strictu (sample KAS). Though sample FMA correspond to sequences previously attributed to the Permian–Triassic Wustkogel Formation of the central Tauern Window (Thiele 1976), the maximum deposition age indicates a more likely affinity with the Seidlwinkel Formation. Furthermore, results are comparable to maximum sedimentation ages of sample MSBG in the footwall of the Glockner Nappe thrust. Alternatively, this sample may be correlated with Late Triassic rocks of the Pfiffkar Formation (Favaro and Schuster 2012).

Despite being scarce, similar results were documented for the meta-arenite of sample MKG (Riffler Basin). The existence of an intercalation of a late Carboniferous metarhyodazite at the base of the Riffler Basin (Fig. 2b, Veselá et al. 2011) implies a protracted sedimentation age for the latter, extending up to the middle to late Triassic.

The obtained late Permian–Triassic maximum deposition ages are also in agreement with the age of the Hochstegen Marble, which overlains post-Variscan metasedimentary sequences of the Tauern Window and yields a late Jurassic Oxfordian age according with fossil content (Schönlaub et al. 1975; Kiessling 1992). Consequently, the studied sequences represent protracted siliciclastic, mainly continental sedimentation, which were afterwards succeeded by a progressive Jurassic marine transgression recorded by

platform deposits of the Hochstegen Marble (Veselá and Lammerer 2008; Veselá et al. 2008).

Surprisingly, sample BSF of the Bündnerschiefer Basin shows only middle Permian maximum sedimentation ages (Table 1), though this unit has been classically assigned to the Jurassic-Cretaceous (e.g., Steinmann 1994; Garofalo 2012). The wide spread of zircon ages may be explained by the existence of a relatively open and deep Penninic Ocean basin (Alpine Tethys), in contrast to underlying sequences (Fig. 2b), thus suggesting a generally low topography and a consequent enlarged catchment area.

In a similar way to maximum deposition ages, provenance is also comparable for most sequences, with main late Carboniferous-Permian and Ordovician-early Silurian peaks. A subordinate, yet relevant Ediacaran contribution is present as well, together with minor input from Archean, Paleoproterozoic, Stenian-Tonian and Cryogenian sources.

Late Carboniferous-Permian ages are attributed to Variscan and post-Variscan magmatism, which is well-documented in the Tauern Window (Söllner et al. 1991; Eichhorn et al. 1999, 2000; Cesare et al. 2002; Kebede et al. 2005; Veselá et al. 2008, 2011). On the other hand, Ordovician-early Silurian zircons possibly derived from Cenerian magmatism (e.g., Zurbriggen 2015, 2017; Oriolo et al. 2021), which is, however, absent in the Tauern Window, despite scarce coeval detrital zircons documented by Kebede et al. (2005). This may imply a more likely derivation from an adjacent tectonostratigraphic domain, where such ages are well-documented (see "Permian–Triassic paleogeography of the Tauern Window").

On the other hand, Ediacaran ages seem to represent a clear Pan-African contribution, being nearly coeval with peak collisional to post-collisional magmatism at ca. 610–580 Ma (e.g., Abdelsalam et al. 2002; Liégeois et al. 2003, 2013; Oriolo et al. 2017). A minor input from Cadomian magmatic sources ubiquitously recorded in pre-Variscan European basement inliers may be feasible as well, particularly for ages between ca. 550–530 Ma (Oriolo et al. 2021 and references therein). Pre-Ediacaran zircons between the Archean and the Cryogenian might have derived from Precambrian sources associated with the northern African crustal blocks, such as the Saharan and Tuareg Shield metacratons (Abdelsalam et al. 2002; Liégeois et al. 2003, 2013). Nevertheless, this may not necessarily imply a derivation from primary Precambrian sources (see "Permian–Triassic paleogeography of the Tauern Window").

Permian–Triassic paleogeography of the Tauern Window

Provenance of the studied late Permian–Triassic metasedimentary sequences provide valuable constraints to reconstruct the paleogeographic position of the Tauern Window during the Variscan to post-Variscan evolution. In the first place, the dominance of late Carboniferous-Permian and Ordovician-early Silurian ages together with the relative scarcity of Precambrian zircons seems to indicate a relatively long-distance from the Gondwana mainland (i.e., northern Africa). Consequently, the most likely source could be attributed to Paleozoic intrusions and their metasedimentary wall rocks, related to the protracted Paleozoic orogenic evolution of the pre-Alpine basement (e.g., Schulz et al. 2008; Siegesmund et al. 2018, 2021; Oriolo et al. 2021). This implies that sediments of Permian–Triassic basins partially resulted from recycling of older (meta) sedimentary sequences.

Ediacaran to Early Paleozoic paleogeographic reconstructions suggested a position of the Tauern Window close to the Bohemian Massif, immediately west/northwest of the Austroalpine and South Alpine units and relatively far away from Gondwana mainland (Ratschbacher and Frisch 1993; Eichhorn et al. 2001; Siegesmund et al. 2021). A roughly comparable paleogeography was also suggested for the Variscan evolution (von Raumer 1998; Eichhorn et al. 2000; Veselá et al. 2011), indicating that the Tauern Window might have been placed between the Austroalpine and South Alpine units, External Alpine units and the Bohemian Massif during the Permian–Triassic, representing one of the easternmost domains of the Penninic units (Fig. 7). Similarities in the provenance of coeval sequences in adjacent

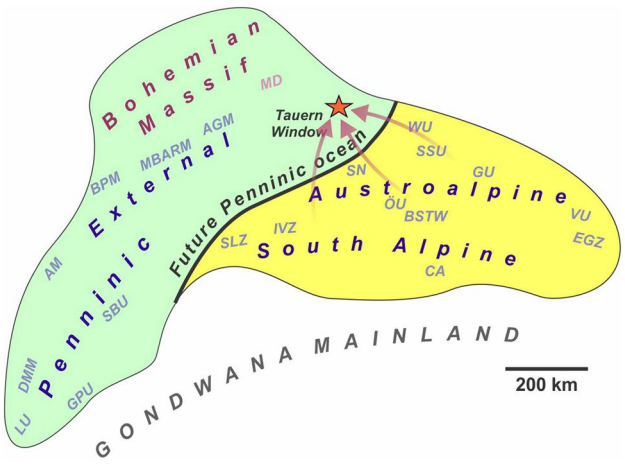

Fig. 7 Sketch showing the position of the Alpine basement domains during the late Permian–Triassic (modified after von Raumer 1998; Haas et al. 2020). *AGM* Aar and Gotthard Massifs, *AM* Argentera Massif, *BPM* Belledonne and Pelvoux Massifs, *BSTW* basement south of the Tauern Window, *CA* Carnic Alps, *DMM* Dora Maira Massif, *EGZ* Eastern Greywacke Zone, *GPU* Gran Paradiso Unit, *GU* Gleinalm Unit, *IVZ* Ivrea-Verbano Zone, *LU* Ligurian Unit, *MBARM* Mont Blanc and Aiguilles Rouges Massifs, *MD* Moldanubian Domain, *ÖU* Ötztal Unit, *SBU* St. Bernhard Unit, *SLZ* Sesia–Lanzo Zone, *SN* Silvretta Nappe, *SSU* Schladming-Seckau Unit, *VU* Veitsch Unit, *WU* Wechsel Unit

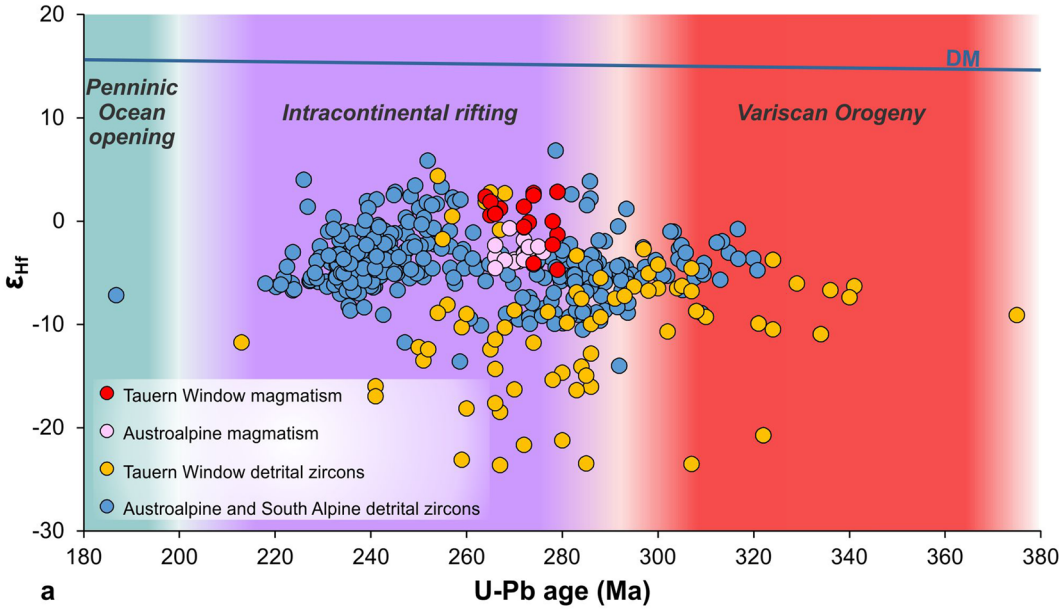
20
10
0
-10
-20
-30
ε_{Hf}
DM
Penninic Ocean opening
Intracontinental rifting
Variscan Orogeny
Tauern Window magmatism
Austroalpine magmatism
Tauern Window detrital zircons
Austroalpine and South Alpine detrital zircons
180
200
220
240
260
280
300
320
340
360
380
U-Pb age (Ma)
a

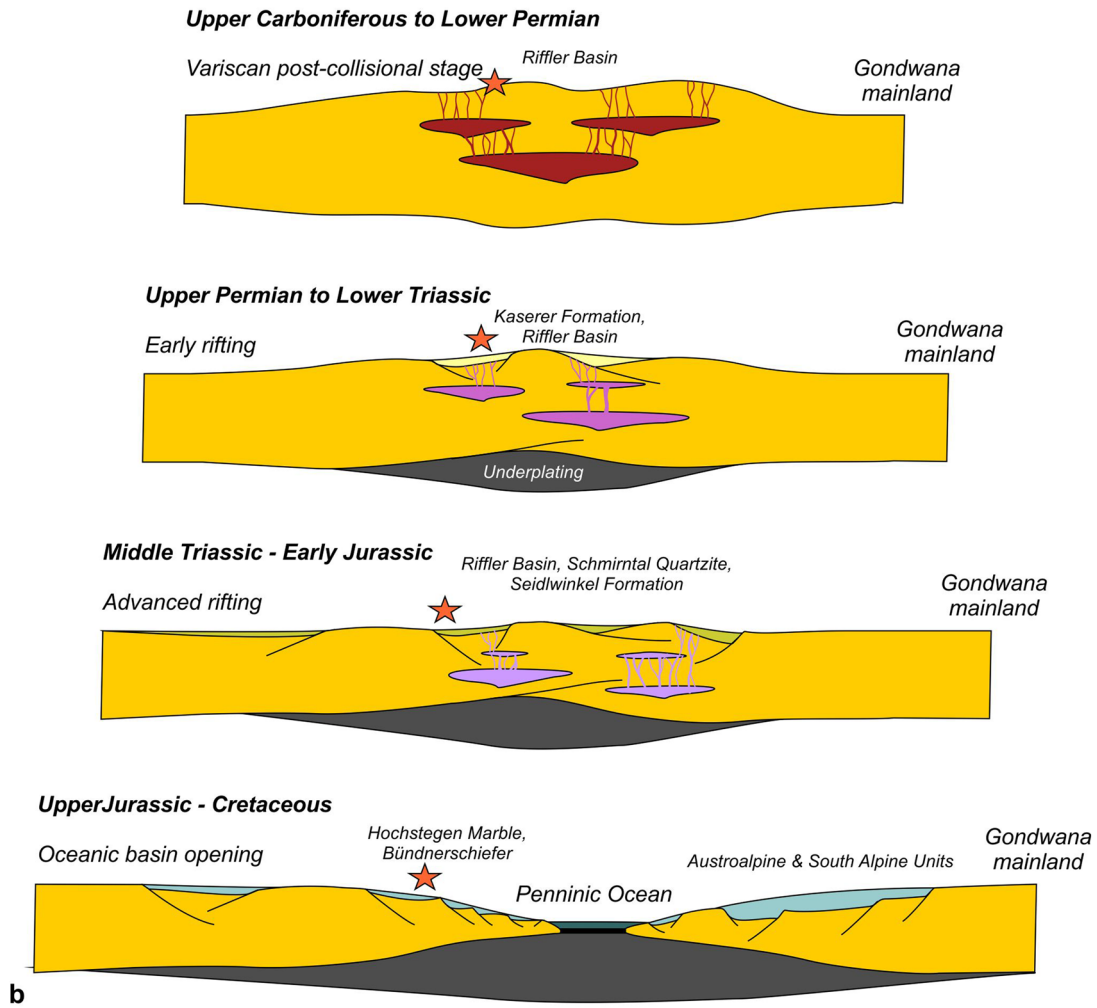
Upper Carboniferous to Lower Permian
Variscan post-collisional stage
Riffler Basin
Gondwana mainland
Upper Permian to Lower Triassic
Early rifting
Kaserer Formation, Riffler Basin
Gondwana mainland
Underplating
Middle Triassic - Early Jurassic
Advanced rifting
Riffler Basin, Schmirntal Quartzite, Seidlwinkel Formation
Gondwana mainland
UpperJurassic - Cretaceous
Oceanic basin opening
Hochstegen Marble, Bündnerschiefer
Austroalpine & South Alpine Units
Gondwana mainland
Penninic Ocean
b

◂**Fig. 8** **a** Compilation of U–Pb vs. ε_{Hf} data of detrital zircons of Permian–Triassic Alpine sequences (Tauern Window magmatic and detrital zircons: this work; Austroalpine and South Alpine detrital zircons: Beltrán-Triviño et al. 2016; Austroalpine magmatic zircons: Yuan et al. 2020). **b** Schematic late to post-Variscan tectonic evolution of the Alpine Units. The star shows the approximate position of the Tauern Window. Studied sequences are indicated

Alpine domains further reinforce this model (Beltrán-Triviño et al. 2016; Wizevich et al. 2019).

Such a paleogeographic position explains the significant recycling of older Paleozoic sequences together with the input of coeval magmatic sources, particularly of those related to the Cenerian orogeny. Though Variscan and even relics of Ediacaran-Cambrian magmatism are well-documented in the Tauern Window (Veselá et al. 2008), Ordovician-early Silurian magmatism is nearly absent, being essentially restricted to amphibolites yielding a U–Pb zircon crystallization ages of ca. 486–482 Ma (von Quadt 1992; Eichhorn et al. 2001) and detrital zircon ages from the Biotitporphyroblastenschiefer (ca. 471–411 Ma) and Felbertal gneisses (ca. 447–405 Ma) (Kebede et al. 2005). However, dominantly felsic peraluminous magmatism and crustal anatexis at ca. 490–450 Ma are well-recorded in the Moldanubian Domain and allochthonous units of the Saxo-Thuringian Domain of the Bohemian Massif (Friedl et al. 2004; Teipel et al. 2004; Sagawe et al. 2016; Koglin et al. 2018; Soejono et al. 2019). Comparable felsic peraluminous magmatism and migmatites yielding ages of ca. 490–440 Ma are also widespread in Austroalpine, South Alpine and Penninic Units (Klötzli-Chowanetz et al. 1997; Meli and Klötzli 2001; Schulz and Bombach 2003; Schulz et al. 2004, 2008; Siegesmund et al. 2007, 2021; Thöny et al. 2008; Bussien et al. 2011; Rode et al. 2012; Cavargna-Sani et al. 2014; Bergomi et al. 2018; Arboit et al. 2019). Furthermore, the peraluminous geochemical signature of the magmatism and the evidence of crustal anatexis explains the dominant subchondritic Lu–Hf composition of Ordovician to early Silurian zircons (Fig. 6).

On the other hand, late Stenian to Tonian zircons, which represent a minor age group in Permian–Triassic sequences, are absent in pre-Variscan metasedimentary rocks of the Tauern Window (Siegesmund et al. 2021). This age group, which is also lacking in Early Paleozoic metasedimentary rocks of the Bohemian Massif, is well documented in coeval Austroalpine and South Alpine sequences (Heinrichs et al. 2012; Siegesmund et al. 2018, 2021). Considering the input of Early Paleozoic magmatism as well, the Austroalpine and South Alpine basement might have thus represented a relatively major source for detritus in Variscan and post-Variscan basins of the Tauern Window.

The narrow age range of the investigated samples and their structural position at the base of the Bündnerschiefer (Penninic nappes) indicate that they formed in a transitional area between the European continental margin and the future Penninic ocean. Deep drilling for the Brenner base tunnel encountered horizons of evaporitic and shallow marine Permian–Triassic strata at several tectonic levels (Brandner 2008; Töchterle et al. 2011). These tectonically weak units served as detachement horizons during Alpine compression and possibly allowed thrusting of the Kaserer Formation over the Hochstegen Marble. Consequently, Permian–Triassic siliciclastic deposits mixed with shallow marine carbonate and evaporitic horizons, Variscan gneiss relics and pre-Variscan mafic and ultramafic basement blocks (metagabbros, amphibolites, serpentinites) may represent a tectonic mélange zone, which originated on a distal and hyperextended continental margin that was imbricated during the Alpine Orogeny.

Pre-Variscan to Variscan tectonosedimentary and magmatic evolution

The earliest record of Variscan magmatic activity in the Tauern Window corresponds to arc granitoids yielding U–Pb SHRIMP zircon ages of ca. 374 Ma (Eichhorn et al. 2000). Subduction culminated at ca. 345–340 Ma during the Variscan collision, triggering crustal anatexis and syncollisional felsic peraluminous intrusions (Finger et al. 1997; Eichhorn et al. 2000), associated with siliciclastic sedimentation (Kebede et al. 2005; Lerchbaumer et al. 2010). Widespread post-collisional magmatism is documented at ca. 340–290 Ma, including the intrusion of durbachitic plutons, which further reinforces the correlation of the Tauern Window with adjacent Alpine basement domains and the Bohemian Massif (e.g., Finger et al. 1997; Veselá et al. 2011; von Raumer et al. 2013; Janoušek et al. 2020). The source of these post-collisional magmas, attributed to a mixing of metasomatized mantle-derived magmas and crustal components, can satisfactorily explain the subchondritic ε_{Hf} values obtained for Carboniferous to early Permian detrital zircons of the studied sequences (Fig. 8).

The change in the isotopic signature of early Permian (< ca. 290 Ma) to middle Triassic detrital zircons, showing a broader spectrum of suprachondritic to subchondritic compositions (Fig. 8a), can be linked to the transition from the Variscan post-collisional stage to a generalized intracontinental extension (Fig. 8b). Protracted Permian to Triassic crustal extension is further supported by the progressive transition from closed intermontane to open sedimentary conditions recorded by geochemical and $\delta^{11}B$ isotopic data of the Permian–Triassic metasedimentary cover of the Western Tauern Window (Franz et al. 2021).

The tectonosedimentary evolution of the studied sequences is comparable to that of late Carboniferous to Triassic deposits of the Pfitsch-Mörchner Basin, characterized by spatially restricted depocenters controlled by horst

and graben structures that are overlapped by the Hochstegen Marble (Veselá and Lammerer 2008; Veselá et al. 2008). Furthermore, coeval South Alpine and Austroalpine units show also a similar history of continental rifting and resulting oceanic basin development, with dominance of Permian–Triassic continental deposits and volcanic and volcaniclastic rocks, succeeded by marine Jurassic deposits (e.g., Bertotti et al. 1993; Cassinis et al. 2012; Beltrán-Triviño et al. 2016).

Lithospheric thinning coupled with magmatic underplating might have triggered rifting-related magmatism and high-temperature/low-pressure metamorphism (Marotta and Spalla 2007; Schuster and Stüwe 2008; Kunz et al. 2018), thus explaining the observed Hf isotopic evolution as the result of mixing of crustal and mantellic sources, which is further supported by Permian magmatism of the Tauern Window and adjacent regions (e.g., Fig. 5; Eichhorn et al. 1999, 2000; Veselá et al. 2011; Yuan et al. 2020). A comparable evolution was also documented for Permian–Triassic volcano-sedimentary sequences of the western South Alpine and Austroalpine Units, based on U–Pb and Lu–Hf detrital zircon data and mineral chemistry of detrital feldspar, spinel and garnet (Beltrán-Triviño et al. 2016). Consequently, late Permian–Triassic metasedimentary rocks of the Tauern Window monitor the progressive transition from Variscan collisional/post-collisional tectonomagmatic processes to intracontinental rifting, which culminated with the opening of the Penninic ocean towards the Jurassic (Fig. 8b; e.g., Ratschbacher et al. 2004; Gleißner et al. 2021).

The presence of scarce zircons yielding anomalously young late Triassic to Jurassic ages (< 210 Ma) may indicate the existence of a post-depositional hydrothermal overprint. Pre-Alpine hydrothermal activity linked to tourmalinite veins was documented by Franz et al. (2021) in the Tauern Window. Though the hydrothermal zircon overprint may be related to these mineralizations, it is unclear whether the obtained zircon ages provide a meaningful temporal constraint for this event.

The Jurassic protolith of the Hochstegen marble was deposited on a marine platform on the subsiding shelf and remains the youngest proven sediment of the Tauern Window. As a post-rift sedimentary sequence, it covers Late Variscan granites gneiss nappes on elevated Variscan highs as well as post-Variscan metasedimentary sequences (Veselá et al. 2008).

Conclusions

Detrital zircon data from metasedimentary rocks of the western Tauern Window yielded maximum deposition ages between the late Permian and the Triassic, indicating protracted sedimentation and magmatism between the Late Paleozoic and the Mesozoic. From a paleogeographical perspective, results indicate that the Tauern Window might have been placed close to further Alpine basement units (South Alpine, Austroalpine and External Massifs) and the Bohemian Massif during the Permian–Triassic, representing one of the easternmost domains of the Penninic Units.

Protracted clastic sedimentation in the Riffler Basin extended between the Late Carboniferous to the Early to Middle Jurassic, and were subsequently covered by Late Jurassic marine deposits of the Hochstegen Marble that covered the entire region. On the other hand, the Kaserer Formation, which is part of the Kaserer nappe, was overthrust by the Hochstegen Marble. Deposition of the Kaserer Formation took place between the late Permian and the Early Triassic, as constrained by Late Permian maximum sedimentation ages and overlying Anisian carbonates and Late Triassic metasiliciclastic sequences of the Seidlwinkel Formation.

In the Glockner Nappe, the lowermost section is characterized by slices of metagabbros and felsic orthogneisses. In this block, metaquarzites and metaconglomerates exposed between the Tuxer Joch to Hintertux, so far attributed to the Wustkogl Formation of the Central Tauern Window, are in fact Late Triassic and seem thus to correlate with sequences of the Seidlwinkel Formation from the Groβglockner area.

The studied sequences, which show similarities with coeval facies of the Germanic Basin, document the transition between Late Paleozoic Variscan post-collisional processes to intracontinental extension. This change possibly occurred at ca. 290, as suggested by variable suprachondritic to subchondritic Lu–Hf compositions of detrital zircons, which contrast with the dominantly subchondritic fingerprint of older zircon crystals. Lithospheric thinning coupled with magmatic underplating might have triggered rifting-related magmatism and high-temperature/low-pressure metamorphism, thus explaining the observed Hf isotopic evolution as the result of mixing of crustal and mantellic sources, which is further supported by Permian magmatism of the Tauern Window and adjacent regions. Progressive intracontinental rifting culminated with the final opening of the Penninic ocean by the Jurassic.

Supplementary Information The online version contains supplementary material available at https://doi.org/10.1007/s00531-022-02179-0.

Acknowledgements We are grateful to the German Research Foundation DFG for financial support of the Project VE 773/1-1. We thank G. Franz, F. Finger and A. von Quadt for their constructive reviews and advices, which helped to improve the final version of this manuscript.

Funding Open Access funding enabled and organized by Projekt DEAL.

References

Abdelsalam MG, Liégeois J-P, Stern RJ (2002) The Saharan Metacraton. J Afr Earth Sci 34:119–136

Arboit F, Chew D, Visoná D, Massironi M, Sciascia F, Benedetti G, Rodani S (2019) The geodynamic evolution of the Italian South Alpine basement from the Ediacaran to the Carboniferous: Was the South Alpine terrane part of the peri-Gondwana arc-forming terranes? Gondwana Res 65:17–30

Baggio P, De Vecchi GP, Mezzacasa G (1982) Carta geologica della media ed alta Valle di Vizze e regione vicine (Alto Adige). B Soc Geol Ital 101:89–116

Beltrán-Triviño A, Winkler W, von Quadt A, Gallhofer D (2016) Triassic magmatism on the transition from Variscan to Alpine cycles: evidence from U–Pb, Hf, and geochemistry of detrital minerals. Swiss J Geosci 109:309–328

Bergomi MA, Dal Piaz GV, Malusà MG, Monopoli B, Tunesi A (2018) The Grand St Bernard-Briançonnais nappe system and the Paleozoic inheritance of the Western Alps unraveled by zircon U–Pb dating. Tectonics 36:2950–2972

Bertotti G, Picotti V, Bernoulli D, Castellarin A (1993) From rifting to drifting: tectonic evolution of the South-Alpine upper crust from the Triassic to the Early Cretaceous. Sediment Geol 86:53–76

Bouvier A, Vervoort JD, Patchett PJ (2008) The Lu–Hf and Sm–Nd isotopic composition of CHUR: Constraints from unequilibrated chondrites and implications for the bulk composition of terrestrial planets. Earth Planet Sci Lett 273:48–57

Brandner R, Reiter F, Töchterle A (2008) Überblick zu den Ergebnissen der geologischen Vorerkundung für den Brenner-Basistunnel. GeoAlp 5:165–174

Bussien D, Bussy F, Magna T, Masson H (2011) Timing of Palaeozoic magmatism in the Maggia and Sambuco nappes and paleogeographic implications (Central Lepontine Alps). Swiss J Geosci 104:1–29

Cassinis G, Perotti CR, Ronchi A (2012) Permian continental basins in the Southern Alps (Italy) and peri-mediterranean correlations. Int J Earth Sci 101:129–157

Cavargna-Sani M, Epard JL, Bussy F, Ulianov A (2014) Basement lithostratigraphy of the Adula nappe: implications for Palaeozoic evolution and Alpine kinematics. Int J Earth Sci 103:61–82

Cesare B, Rubatto D, Hermann J, Barzi L (2002) Evidence for Late Carboniferous subduction-type magmatism in mafic-ultramafic cumulates of the SW Tauern window (Eastern Alps). Contrib Mineral Petrol 142:449–464

Coutts DS, Matthews WA, Hubbard SM (2019) Assessment of widely used methods to derive depositional ages from detrital zircon populations. Geosci Front 10:1421–1435

De Min A, Velicogna M, Ziberna L, Chiaradia M, Alberti A, Marzoli A (2020) Triassic magmatism in the European Southern Alps as an early phase of Pangea break-up. Geol Mag 157:1800–1822

Dickinson WR, Gehrels GE (2009) Use of U–Pb ages of detrital zircons to infer maximum depositional ages of strata: a test against a Colorado Plateau Mesozoic database. Earth Planet Sci Lett 288:115–125

Doglioni C (1987) Tectonics of the Dolomites (southern Alps, northern Italy). J Struct Geol 9:181–193

Eichhorn R, Höll R, Loth G, Kennedy A (1999) Implications of U–Pb SHRIMP zircon data on the age and evolution of the Felbertal tungsten deposit (Tauern Window, Austria). Int J Earth Sci 88:496–512

Eichhorn R, Loth G, Höll R, Finger F, Schermaier A, Kennedy A (2000) Multistage Variscan magmatism in the central Tauern Window (Austria) unveiled by U/Pb SHRIMP zircon data. Contrib Mineral Petrol 139:418–435

Eichhorn R, Loth G, Kennedy A (2001) Unravelling the pre-Variscan evolution of the Habach terrane (Tauern Window, Austria) by U–Pb SHRIMP zircon data. Contrib Mineral Petrol 142:147–162

Favaro S, Schuster R (2012) Bericht 2012 über geologische Aufnahmen auf den Blättern 154 Rauris, 155 Bad Hofgastein, 181 Obervellach. Jahrb Geolog Bundesanstalt Wien 152:268–272

Fenti V, Friz L (1973) Il progetto de la galleria ferroviaria Vipiteno-Innsbruck (versante italiano). I. Ricerche geostrutturali sulla regione del Brennero. Mem Mus Trid Sc Nat 20:1–59

Finger F, Roberts MP, Haunschmid B, Schermaier A, Steyrer HP (1997) Variscan granitoids of central Europe: their typology, potential sources and tectonothermal relations. Mineral Petrol 61:67–96

Franz G, Kutzschbach M, Berryman EJ, Meixner A, Loges A, Schultze D (2021) Geochemistry and paleogeographic implications of Permo-Triassic metasedimentary cover from the Tauern Window (Eastern Alps). Eur J Mineral 33:401–423

Frasl G (1958) Zur Seriengliederung der Schieferhülle in den mittleren Hohen Tauern. Geologische Bundesanstalt Jahrb Geolog Bundesanstalt Wien 101:323–473

Friedl G, Finger F, Paquette JL, von Quadt A, McNaughton NJ, Fletcher IR (2004) Pre-Variscan geological events in the Austrian part of the Bohemian Massif deduced from U–Pb zircon ages. Int J Earth Sci 93:802–823

Frisch W (1974) Die stratigraphisch-tektonische Gliederung der Schieferhülle und die Entwicklung des penninischen Raumes im westlichen Tauernfenster (Gebiet Brenner—Gerlospaß). Mitt Geol Ges Wien 66–67:9–20

Frisch W (1975) Ein Typ-Profil durch die Schieferhülledes Tauernfensters: Das Profil am Wolfendorn (westlicher Tuxer Hauptkamm, Tirol). Verhandlungen Der Geologischen Bundesanstalt 1974:201–221

Frisch W, Dunkl I, Kuhlemann J (2000) Post-collisional orogenparallel large-scale extension in the Eastern Alps. Tectonophysics 327:239–265

Garofalo PS (2012) The composition of Alpine marine sediments (Bündnerschiefer Formation, W Alps) and the mobility of their chemical components during orogenic metamorphism. Lithos 128:55–72

Gleißner P, Franz G, Frei D (2021) Contemporaneous opening of the Alpine Tethys in the Eastern and Western Alps: constraints from a Late Jurassic gabbro intrusion age in the Glockner Nappe, Tauern Window, Austria. Int J Earth Sci. https://doi.org/10.1007/s00531-021-02075-z

Haas I, Eichinger S, Haller D, Fritz H, Nievoll J, Mandl M, Hippler D, Hauzenberger C (2020) Gondwana fragments in the Eastern Alps: a travel story from U/Pb zircon data. Gondwana Res 77:204–222

Heinrichs T, Siegesmund S, Frei D, Drobe M, Schulz B (2012) Provenance signatures from whole-rock geochemistry and detrital zircon ages of metasediments from the Austroalpine basement south of the Tauern Window (Eastern Tyrol, Austria). Geo Alp 9:156–185

Höck V, Miller C (1980) Chemistry of mesozoic metabasites in the middle and eastern part of the Hohe Tauern. Mitt Österr Geol Ges 71(72):81–88

Janoušek V, Hanžl P, Svojtka M, Hora JM, Kochergina YVE, Gadas P, Holub FV, Gerdes A, Verner K, Hrdličková K, Daly JS, Buriánek D (2020) Ultrapotassic magmatism in the heyday of the Variscan Orogeny: the story of the Třebíč Pluton, the largest durbachitic body in the Bohemian Massif. Int J Earth Sci 109:1767–1810

Kebede T, Klötzli U, Kosler J, Skiöld T (2005) Understanding the pre-Variscan and Variscan basement components of the central Tauern Window, Eastern Alps (Austria): constraints from single zircon U–Pb geochronology. Int J Earth Sci 94:336–353

Kiessling W (1992) Palaeontological and facial features of the Upper Jurassic Hochstegen marble (Tauern window, Eastern Alps). Terra Nova 4:184–197

Klötzli-Chowanetz E, Klötzli U, Koller F (1997) Lower Ordovician migmatization in the Ötztal crystalline basement (Eastern Alps, Austria): linking U–Pb and Pb–Pb dating with zircon morphology. Schweiz Miner Petrog Mitt 77:315–324

Koglin N, Zeh A, Franz G, Schüssler U, Glodny J, Gerdes A, Brätz H (2018) From Cadomian magmatic arc to Rheic ocean closure: the geochronological-geochemical record of nappe protoliths of the Münchberg Massif, NE Bavaria (Germany). Gondwana Res 55:135–152

Kunz BE, Manzotti P, von Niederhäusern B, Engi M, Darling JR, Giuntoli F, Lanari P (2018) Permian high-temperature metamorphism in the Western Alps (NW Italy). Int J Earth Sci 107:203–229

Kurz W, Neubauer F, Genser J, Dachs E (1998) Alpine geodynamic evolution of passive and active continental margin sequences in the Tauern Window (eastern Alps, Austria, Italy): a review. Geol Rundsch 87:225–242

Lammerer B, Weger M (1998) Footwall uplift in an orogenic wedge: the Tauern Window in the Eastern Alps of Europe. Tectonophysics 285:213–230

Lammerer B, Gebrande H, Lüschen E, Vesela P (2008) A crustal-scale cross-section through the Tauern Window (eastern Alps) from geophysical and geological data. In: Siegesmund S, Fügenschuh B, Froitzheim N (eds) Tectonic aspects of the Alpine–Dinaride–Carpathian system, vol 298. Geological Society, London, pp 219–229

Lemcke K (1988) Das Bayerische Alpenvorland vor der Eiszeit. Geologie von Bayern. Schweizerbart´sche Verlagsbuchhandlung, Stuttgart

Lerchbaumer L, Kloetzli U, Pestal G (2010) Schists and amphibolites of the Kleinelendtal (Ankogel-Hochalm-Gruppe/Hohe Tauern, Austria)/new insights on the Variscan basement in the Eastern Tauern Window. Austrian J Earth Sci 103:138–152

Liégeois JP, Latouche L, Boughrara M, Navez J, Guiraud M (2003) The LATEA metacraton (Central Hoggar, Tuareg shield, Algeria): behaviour of an old passive margin during the Pan-African orogeny. J Afr Earth Sci 37:161–190

Liégeois J-P, Abdelsalam MG, Ennih N, Ouabadi A (2013) Metacraton: nature, genesis and behavior. Gondwana Res 23:220–237

Manzotti P, Rubatto D, Zucali M, El Korh A, Cenki-Tok B, Ballevre M, Engi M (2018) Permian magmatism and metamorphism in the Dent Blanche nappe: constraints from field observations and geochronology. Swiss J Geosci 111:79–97

Marotta AM, Spalla MI (2007) Permian-Triassic high thermal regime in the Alps: result of late Variscan collapse or continental rifting? Validation by numerical modeling. Tectonics 26:TC4016

Meli S, Klötzli US (2001) Evidence for Lower Paleozoic magmatism in the Eastern Southalpine basement: zircon geochronology from Comelico porphyroids. Schweiz Miner Petrog Mitt 81:147–157

Oriolo S, Oyhantçabal P, Wemmer K, Siegesmund S (2017) Contemporaneous assembly of Western Gondwana and final Rodinia break-up: implications for the supercontinent cycle. Geosci Front 8:1431–1445

Oriolo S, Schulz B, Geuna S, González PD, Otamendi JE, Sláma J, Druguet E, Siegesmund S (2021) Early Paleozoic accretionary orogens along the Western Gondwana margin. Geosci Front 12:109–130

Quick JE, Sinigoi S, Peressini G, Demarchi G, Wooden JL, Sbisà A (2009) Magmatic plumbing of a large Permian caldera exposed to a depth of 25 km. Geology 37:603–606

Ratschbacher L, Frisch W (1993) Palinspastic reconstruction of the pre-triassic basement units in the Alps: the Eastern Alps. In: Raumer JFV, Neubauer F (eds) Pre-mesozoic geology in the Alps. Springer, Heidelberg, pp 41–51

Ratschbacher L, Frisch W, Neubauer F, Schmid SM, Neugebauer J (1989) Extension in compressional orogenic belts: The Eastern Alps. Geology 17:404–407

Ratschbacher L, Dingeldey C, Miller C, Hacker BR, McWilliams MO (2004) Formation, subduction, and exhumation of Penninic oceanic crust in the Eastern Alps: time constraints from $^{40}Ar/^{39}Ar$ geochronology. Tectonophysics 394:155–170

Rockenschaub M, Kolenprat B, Nowotny A (2003) Das westliche Tauernfenster. Arbeitstagung Geolog Bundesanstalt Wien 148:7–38

Rode S, Rösel D, Schulz B (2012) Constraints on the Variscan P–T evolution by EMP Th–U–Pb monazite dating in the polymetamorphic Austroalpine Oetztal-Stubai basement (Eastern Alps). Z Dtsch Ges Geowiss 163:43–67

Rosenberg CL, Brun JP, Cagnard F, Gapais D (2007) Oblique indentation in the Eastern Alps: insights from laboratory experiments. Tectonics 26:TC2003

Sagawe A, Gärtner A, Linnemann U, Hofmann M, Gerdes A (2016) Exotic crustal components at the northern margin of the Bohemian Massif—implications from U–Th–Pb and Hf isotopes of zircon from the Saxonian Granulite Massif. Tectonophysics 681:234–249

Satterley AK (1996) The interpretation of cyclic successions of the Middle and Upper Triassic of the Northern and Southern Alps. Earth Sci Rev 40:181–207

Schmid SM, Scharf A, Handy MR, Rosenberg CL (2013) The Tauern Window (Eastern Alps, Austria): a new tectonic map, with cross-sections and a tectonometamorphic synthesis. Swiss J Geosci 106:1–32

Schulz B, Bombach K (2003) Single zircon Pb–Pb geochronology of the early-Palaeozoic magmatic evolution in the Austroalpine basement to the south of the Tauern Window. Jahrb Geol BA 143:303–321

Schulz B, Bombach K, Pawlig S, Brätz H (2004) Neoproterozoic to early-Palaeozoic magmatic evolution in the Gondwana-derived Austroalpine basement to the south of the Tauern Window (Eastern Alps). Int J Earth Sci 93:824–843

Schulz B, Steenken A, Siegesmund S (2008) Geodynamic evolution of an Alpine terrane—the Austroalpine basement to the south of the Tauern window as a part of the Adriatic Plate (eastern Alps). In: Siegesmund S, Fügenschuh B, Froitzheim N (eds) Tectonic aspects of the Alpine–Dinaride–Carpathian system, vol 298. Geological Society, London, pp 5–44

Schuster R, Stüwe K (2008) Permian metamorphic event in the Alps. Geology 36:603–606

Selverstone J (1985) Petrologic constraints on imbrication, metamorphism, and uplift in the SW Tauern window, Eastern Alps. Tectonics 4:687–704

Selverstone J (1988) Evidence for east-west crustal extension in the eastern Alps: implications for the unroofing history of the Tauern Window. Tectonics 7:87–105

Selverstone J, Spear FS, Franz G, Morteani G (1984) High-pressure metamorphism in the SW Tauern Window, Austria: P–T paths from hornblende-kyanite-staurolite schists. J Petrol 25:501–531

Selverstone J, Axen GJ, Bartely JM (1995) Fluid inclusion constraints on the kinematics of footwall uplift beneath the Brenner Line normal fault, Eastern Alps. Tectonics 14:264–278

Siegesmund S, Heinrichs T, Romer RL, Doman D (2007) Age constraints on the evolution of the Austroalpine basement to the south of the Tauern Window. Int J Earth Sci 96:415–432

Siegesmund S, Oriolo S, Heinrichs T, Basei MAS, Nolte N, Hüttenrauch F, Schulz B (2018) Provenance of Austroalpine basement metasediments: tightening up Early Palaeozoic connections between peri-Gondwanan domains of central Europe and Northern Africa. Int J Earth Sci 107:2293–2315

Siegesmund S, Oriolo S, Schulz B, Heinrichs T, Basei MAS, Lammerer B (2021) The birth of the Alps: Ediacaran to Paleozoic accretionary processes and crustal growth along the northern Gondwana margin. Int J Earth Sci. https://doi.org/10.1007/s00531-021-02019-7

Söderlund U, Patchett PJ, Vervoort JD, Isachsen CE (2004) The ^{176}Lu decay constant determined by Lu–Hf and U–Pb isotope systematics of Precambrian mafic intrusions. Earth Planet Sci Lett 219:311–324

Schönlaub HP, Frisch W, Flajs G (1975) Neue Fossilfunde aus dem Hochstegenmarmor (Tauernfenster, österreich). N Jb Geol Paläont Mh 1974:111–128

Soejono I, Machek M, Sláma J, Janoušek V, Kohút M (2019) Cambro-Ordovician anatexis and magmatic recycling at the thinned Gondwana margin: new constraints from the Kouřim Unit, Bohemian Massif. J Geol Soc 177:325–341

Söllner F, Höll R, Miller H (1991) U–Pb-Systematik der Zirkone in Meta-Vulkaniten (“‘Porphyroiden”’) aus der Nördlichen Grauwackenzone und dem Tauernfenster (Ostalpen, Österreich). Z Dtsch Geol Ges 142:285–299

Steinmann M (1994) Ein Beckenmodell fur das Nordpenninikum der Ostschweiz. Jahrb Geol BA 137:675–721

Storck JC, Brack P, Wotzlaw JF, Ulmer P (2019) Timing and evolution of Middle Triassic magmatism in the Southern Alps (northern Italy). J Geol Soc 176:253–268

Teipel U, Eichhorn R, Loth G, Rohrmüller J, Höll R, Kennedy A (2004) U–Pb SHRIMP and Nd isotopic data from the western Bohemian Massif (Bayerischer Wald, Germany): implications for upper Vendian and lower Ordovician magmatism. Int J Earth Sci 93:782–801

Thiele O (1976) Der Nordrand des Tauernfensters zwischen Mayrhofen und Inner Schmirn (Tirol). Geol Rundschau 65:410–421

Thöny WF, Tropper P, Schennach F, Krenn E, Finger F, Kaindl R, Franz B, Hoinkes G (2008) The metamorphic evolution of migmatites from the Ötztal Complex (Tyrol, Austria) and constraints on the timing of the pre-Variscan high-T event in the Eastern Alps. Swiss J Geosci 101:111–126

Töchterle A, Brandner R, Reiter F (2011) Strain partitioning on major fault zones in the northwestern Tauern Window—insights from the investigations of the Brenner base tunnel. Austrian J Earth Sci 104:15–35

Tollmann A (1977) Geologie von Österreich. Die Zentralalpen, Deuticke

Vermeesch P (2012) On the visualization of detrital age distributions. Chem Geol 312–313:190–194

Vervoort JD, Blichert-Toft J (1999) Evolution of the depleted mantle: Hf isotope evidence from juvenile rocks through time. Geochim Cosmochim Acta 63:533–556

Veselá P, Lammerer B (2008) The Pfitsch-Mörchner Basin, an example of the post-Variscan sedimentary evolution in the Tauern Window (Eastern Alps). Swiss J Geosci 101:73–88

Veselá P, Lammerer B, Wetzel A, Söllner F, Gerdes A (2008) Post-Variscan to Early Alpine sedimentary basins in the Tauern Window (eastern Alps). In: Siegesmund S, Fügenschuh B, Froitzheim N (eds) Tectonic aspects of the Alpine–Dinaride–Carpathian system, vol 298. Geological Society, London, pp 83–100

Veselá P, Söllner F, Finger F, Gerdes A (2011) Magmato-sedimentary Carboniferous to Jurassic evolution of the western Tauern window, Eastern Alps (constraints from U-Pb zircon dating and geochemistry). Int J Earth Sci 100:993–1027

von Quadt A (1992) U–Pb zircon and Sm–Nd geochronology of mafic and ultramafic rocks from the central part of the Tauern Window (Eastern Alps). Contrib Mineral Petrol 110:57–67

von Raumer JF (1998) The Palaeozoic evolution in the Alps: from Gondwana to Pangea. Geol Rundsch 87:407–435

von Raumer JF, Bussy F, Stampfli GM (2009) The Variscan evolution in the external massifs of the Alps and place in their Variscan framework. Comptes Rendus Geosci 341:239–252

von Raumer JF, Bussy F, Schaltegger U, Schulz B, Stampfli GM (2013) Pre-Mesozoic Alpine basements—their place in the European Paleozoic framework. Geol Soc Am Bull 125:89–108

Wizevich MC, Meyer CA, Linnemann U, Gärtner A, Sonntag BL, Hofmann M (2019) U-Pb zircon provenance of Triassic sandstones, western Swiss Alps: implications for geotectonic history. Swiss J Geosci 112:419–434

Yuan S, Neubauer F, Liu Y, Genser J, Liu B, Yu S, Chang R, Guan Q (2020) Widespread Permian granite magmatism in Lower Austroalpine units: significance for Permian rifting in the Eastern Alps. Swiss J Geosci 113:1–25

Zurbriggen R (2015) Ordovician orogeny in the Alps: a reappraisal. Int J Earth Sci 104:335–350

Zurbriggen R (2017) The Cenerian orogeny (early Paleozoic) from the perspective of the Alpine region. Int J Earth Sci 106:517–529